Supporting Information

Towards a droplet radiometric assay for single-cell analysis

Maria Elena Gallina[a,1], Tae Jin Kim[a,1], Mark Shelor[b], Jaime Vasquez[c], Amy Mongersun[e], Minkyu Kim[d], Sindy K. Y. Tang[d], Paul Abbyad[e], Guillem Pratx[a,*]

[a]*Division of Medical Physics, Department of Radiation Oncology, Stanford University,300 Pasteur Drive, Stanford, CA 94305, USA*

[b]*University of California-Merced, Department of Bioengineering, Merced 5200 North Lake Rd., Merced, CA, 95343, USA*

[c]*University of California-San Francisco, School of Pharmacy, 600 16th Street, San Francisco, 94158, USA*

[d]*Department of Mechanical Engineering, Stanford University, 418 Panama Mall, Stanford, 94305, USA*

[e]*Department of Chemistry and Biochemistry, Santa Clara University, Daly Science 123500 El Camino Real, Santa Clara, 95053, USA*

[*] Corresponding author. Tel.: +1 650 724 9829; fax: +1 650 723 7254.

E-mail address: pratx@stanford.edu

[1] These authors contributed equally to the work.

Table of contents

Dose [Gy]	Mean Intensity [A.U.]	Standard Deviation (σ)
0	240	50
4	715	130
8	100	240
12	1290	295

Table S1. Background-corrected mean intensity values and corresponding standard deviations for single droplets exposed to different X-ray doses (Figure 3b). Increase in mean droplet intensity in response to X-ray was evaluated by linear regression ($R^2 > 0.97$): $\langle I \rangle = 297 + (86\ \mathrm{Gy}^{-1}) \cdot \mathrm{Dose}$.

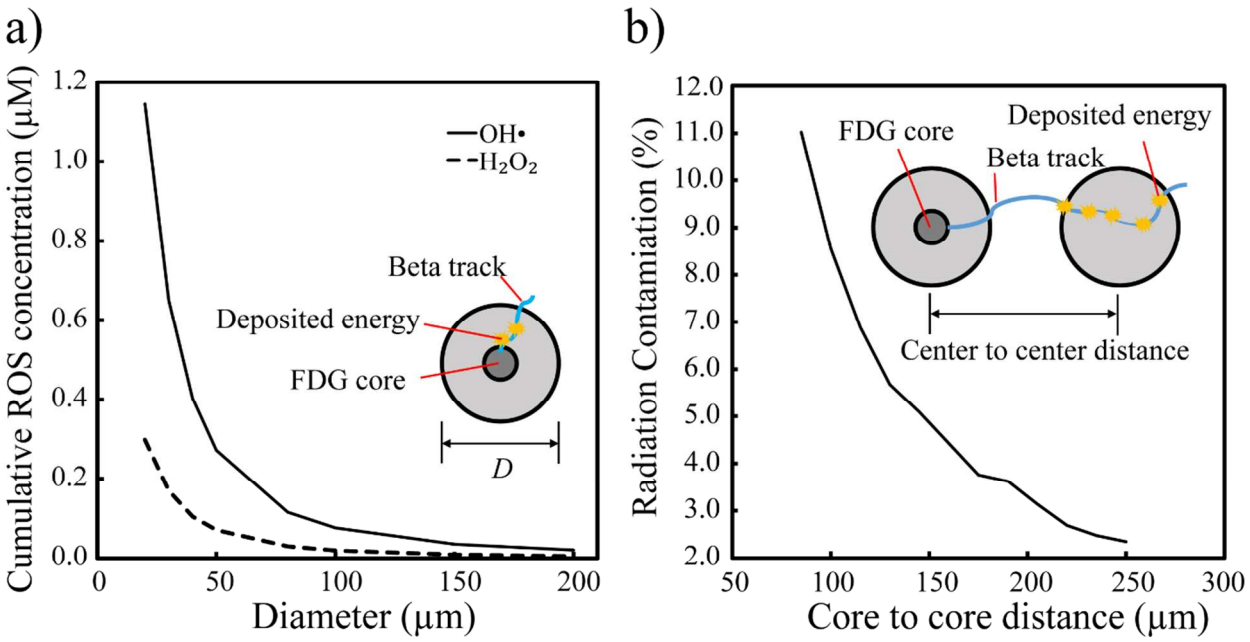

Figure S1. Monte Carlo simulations. a) Droplet size effects: the simulated cell (labeled "FDG core") is modeled as a sphere (diameter, 10 μm) filled with 10 Bq of ^{18}F contained inside a larger spherical water droplet with variable diameter. The cumulative ROS concentration is calculated based on the total energy deposited in the droplet for 4 hours and water radiolysis yields ($^{\bullet}OH$: 0.28 μmol/J; H_2O_2: 0.073 μmol/J). b) Radiation cross-contamination: a sphere mimicking a radiolabeled cell (diameter, 10 μm) is encapsulated in a water droplet (diameter, 85 μm), and an empty droplet (diameter, 85 μm) is placed in a variable distance from the radioactive droplet. The contamination ratio is measured by normalizing the energy deposited in the blank droplet by the energy deposited in the droplet with the radioactive source.

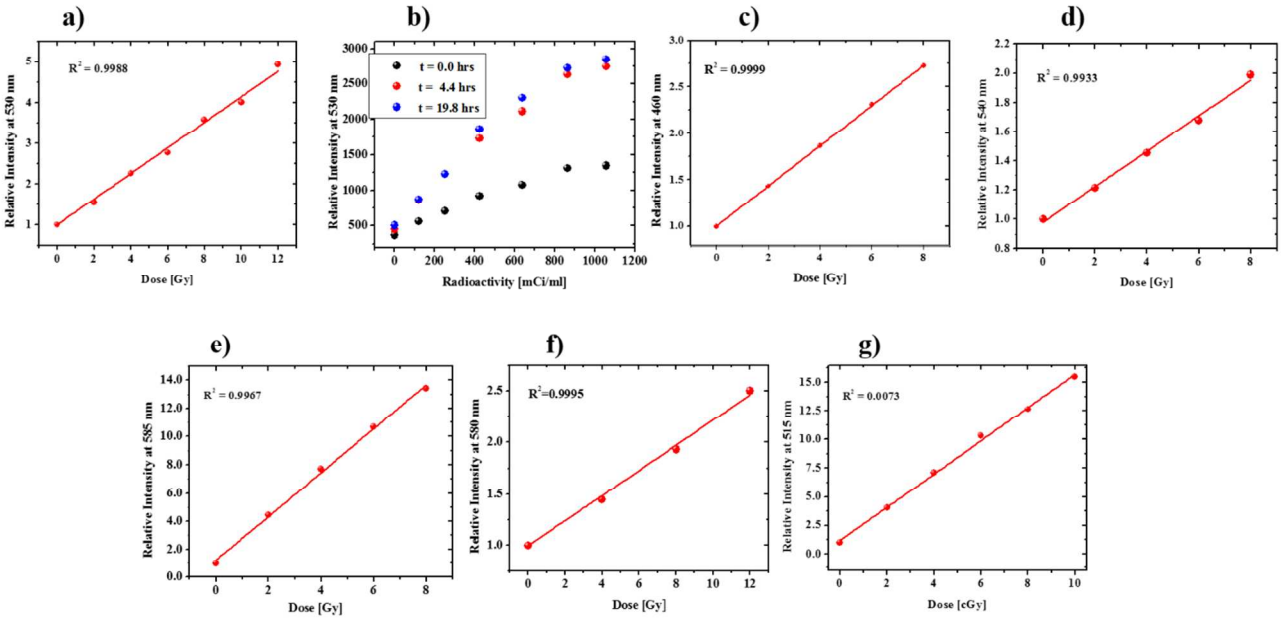

Figure S2. Radiation response of multiple ROS sensors dissolved in PBS, with corresponding linear regression: (a) SOSG, (c) Coumarin C3C, (d) 2′, 7′-Dichlorofluorescin diacetate, (e) Amplex Red, (f) ROS Star 550, and (g) APF. Concentrations are reported in Table 1. (b) Fluorescence activation of SOSG 10 µM in PBS as a function of [^{18}F]FDG activity concentration at different times after addition of the radiotracer. Intensity variations are stabilized after 4.4 hours and they remain stable for at least 20 hrs. At the working concentration (10 µM), the linear response saturates at ca. 800 µCi/ml.

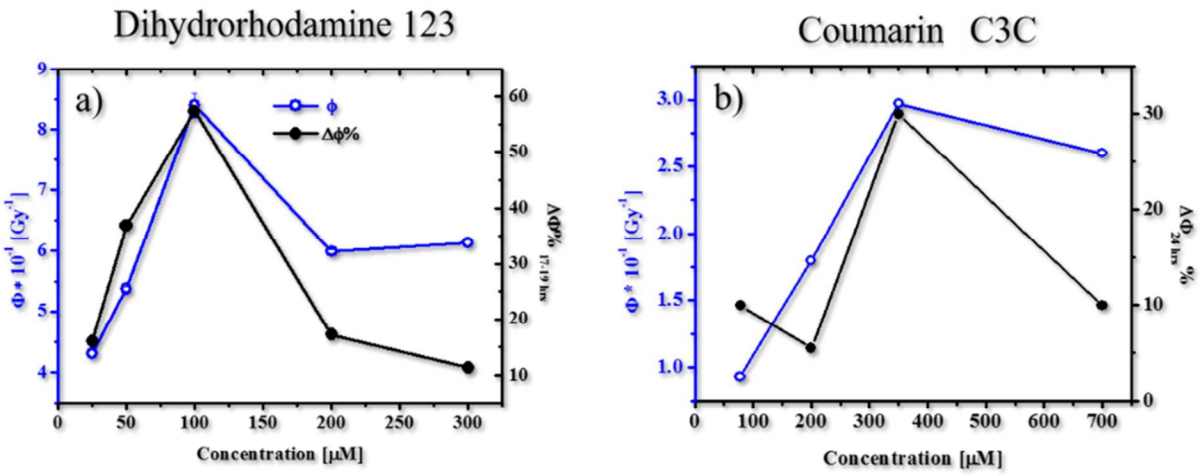

Figure S3. Effect of ROS sensor concentration. a) Sensitivity (Φ, blue) and stability (ΔΦ%, black) of DHRh 123 as a function of concentration. b) Same as previous, for C3C. Sensitivity is estimated by exposing the sensor to increasing doses of X-ray and measuring the slope of the resulting fluorescent response (see Figure 2 for details). Stability, evaluated here as the percentage drop in sensitivity after a defined amount of time, is also a function of sensor concentration. DHRh 123 concentration was kept constant at 200 μM in all other experiments as it presents the best compromise between sensitivity and stability.

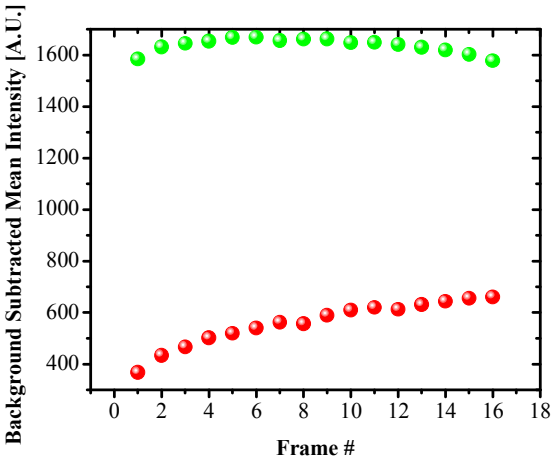

Figure S4. Change in fluorescence intensity over time in droplets containing DHRh 123 (200 μM), measured by fluorescence microscopy. Red and green dots represent the mean intensity values of a non-irradiated and irradiated (12 Gy, X-ray) droplet, respectively. Frames were taken every 15 minutes.

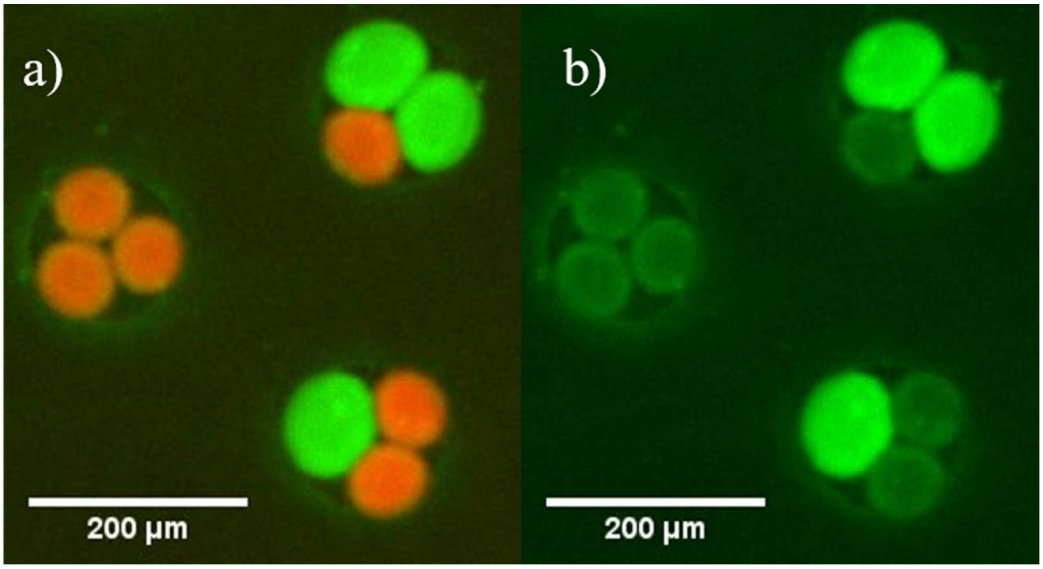

Figure S5. Fluorescence microscopy images of droplets containing DHRh 123 (200 µM), mixed with either ^{18}F-FDG (1.0 mCi/ml) or Alexa 594 (0.0 mCi/ml). a) Superposition of GFP and Texas-Red channels, showing that activation of DHRh 123 only occurs in droplets containing [^{18}F]FDG. (b) GFP channel only, showing absence of physical cross-contamination, even between adjacent droplets trapped on the same anchor.